

# Outage Probability Analysis of Wireless Energy Harvesting-Assisted Networks Considering Dual Energy-Data Channel Models

S. Poursheikhali

Chabahar Maritime University, Chabahar, Iran.

Received Date 21 April 2022; Revised Date 28 April 2022; Accepted Date 30 April 2022

\*Corresponding author: s.poursheikhali@cmu.ac.ir (S. Poursheikhali)

## Abstract

In this work, an energy harvesting-assisted wireless network is considered, where a source, contrary to the conventional networks, harvests its required energy via two independent energy channels. In addition, we assume a destination terminal, which receives the interference signals along with the data transferred by the source. In this model, the source is considered to scavenge energy from the destination's broadcasted signal and ambient interference signal. We model the energy and data channels via the Rayleigh-Rician channel model. Then the system outage probability is obtained after analyzing the outage probability of energy and data channels. Moreover, another scenario in which the source is assumed to harvest energy from only the destination terminal is investigated. The computer simulations are conducted in order to evaluate the effectiveness of the proposed approach, and the impacts of different system parameters on the system outage probability are investigated. The results obtained indicate the outperformance of the scenario in which energy harvests via two channels compared to the case where only one energy harvesting channel exists. In addition, the overall system outage highly degrades when outage in energy channels decreases, especially in the first scenario.

**Keywords:** Energy harvesting; Outage probability; Radio frequency; Wireless energy transfer.

## 1. Introduction

Wireless has only been used for communications via radio frequency (RF) radiation for a long time. However, the recent research works go beyond the conventional communication-centric transmission. Powering devices via wireless radiation brings new opportunities including no need for wires and batteries, energy efficiency, and increased devices' lifetime. In the low-power wireless applications such as wireless sensor networks (WSNs) and the internet of things (IoT), energy harvesting (EH) is a good substitute for the traditional battery because the operational lifetime of rechargeable batteries is limited, and replacing the sensors' exhausted batteries is not viable in these high-density networks. However, through the EH approaches, the lifetime of a network can be extended, and the maintenance cost is minimized. The EH techniques enable low-power devices to scavenge energy from various sources. Besides the conventional renewable energy sources such as thermal, solar, and wind, RF signal radiated by ambient transmitters are considered as a new source for energy harvesting.

The wireless-powered communication networks (WPCNs) are the wireless networks that take advantage of both information and energy carried by radio signals [1]. Wireless terminals typically have no internal energy supply in these networks, and are powered by wireless energy transfer (WET). WET and wireless information transfer (WIT) are performed separately in a WPCN, as in [2]. Here, a hybrid access point broadcasts energy in the downlink, and receives information in the uplink. In general, WPCNs have been studied over various setups. An overview of the networking structures, techniques to build an efficient WPCN, and challenges are presented in [3]. A novel harvest-then-transmit protocol for WPCN has been proposed in [4], which examines the sum throughput maximization. In [5], the outage probability, achievable throughput, ergodic capacity, and bit error rate (BER) of a WPCN under the generalized  $\kappa - \mu$  fading model are derived. The average throughput analysis of a WPC system under Rayleigh and Nakagami- $m$  fading channel has been investigated in [6] and

[7], respectively. Moreover, many studies, i.e. [8]-[13], address the wireless energy harvesting issue. In most studies, it is considered that the WET channels provide a constant amount of energy permanently. However, this assumption does not hold in most applications, as the WET channels may be subject to an outage. In [14], the data and energy channels have been considered separately, and the authors have proposed a new transmission scheduling. The outage probability analysis of a relay-assisted energy transmission scenario has been investigated in [15]. Here, it is considered that the transmitter is powered via two links, a direct and a link equipped with an energy harvesting relay. Then an energy-efficient scheduling method is proposed based on the energy and data channel outage probabilities.

Based on the above studies, in this work, we investigate the outage of a WPCN in the presence of interference signals under the Rician-Rayleigh fading channel model. A time switching-based protocol is applied for energy harvesting and data transfer. In the first phase of a transmission block, the source terminal conducts RF energy harvesting. The required energy of the source is assumed to provide via two independent channels, from both the destination terminal and the interference signal from the ambient. After finishing the energy harvesting phase, the source transmits data by applying the stored energy during the second phase. The environmental interference signals also affect the received signal at the destination. In this model, the aim is to analyze the system outage probability regarding the outage of energy channels. In addition, another scenario is considered to examine the impact of the amount of harvest energy on the system performance. Thus in the second scenario, the source is considered to scavenge energy via only one channel. Moreover, the simulations are conducted in order to evaluate the system's performance.

The rest of this paper is organized as what follows. The explanation of the proposed system model is presented in Section 2. The outage probability analysis of the system is discussed in Section 3. Section 4 investigates a special case of the proposed model in which the source harvests energy from only one energy channel. Section 5 is specified for simulations. Finally, the paper is concluded in Section 6.

**2. System model**

In this work, a scenario with four point-to-point channels including  $D \rightarrow S, I \rightarrow S, S \rightarrow D, I \rightarrow D$  is considered, as illustrated in figure 1 (a).

Subscript-S is applied for the source terminal, subscript-D for the destination terminal, and subscript-I for the interference signal. Both the source and destination terminals are assumed to have a single antenna. The energy harvesting and data transmission links are presented by dashed and solid lines, respectively. As demonstrated in figure 1 (b), the considered model has two phases during each transmission block with a time length  $T$ . The first phase of the block is  $\alpha T$  amount of time, where  $\alpha$  denotes the time-splitting factor for energy harvesting and data transfer, and is as  $0 < \alpha < 1$ . As depicted in figure 1(b), the energy harvesting process is performed in the first phase. It should be noted that the source terminal is considered to have no internal energy supply, and provides its energy via scavenging RF energy from two independent links,  $I \rightarrow S$  and  $D \rightarrow S$ . In general, the interference signals are considered undesirable for the data channels as it degrades their performance by affecting the signal-to-noise ratio. However, the interference may be helpful for energy channels as it boosts the aggregate energy. In the considered model, it is assumed that the source terminal makes use of the interference by harvesting and storing the broadcasted RF energy over the  $I \rightarrow S$  link. The stochastic nature of the ambient RF signal makes it intermittent. Thus to be more reliable, the source is assumed to harvest the RF energy from the destination over *the*  $D \rightarrow S$  link. The second phase, with a time length  $(1 - \alpha)T$ , is specified for the data transfer. During this time interval, the destination is received data over two links. The powered source transfers data to the destination over the  $S \rightarrow D$  link. It is assumed that the source uses all the energy stored during the first phase for transferring the data. Simultaneously, the ambient interference signal is received by the destination over the  $I \rightarrow D$  link.

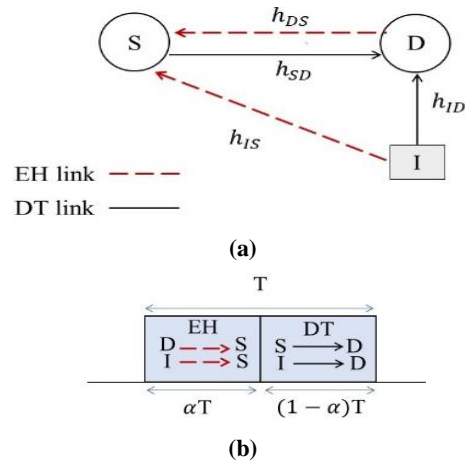


**Figure 1. Wireless powered communication network (a) system model, (b) transmission block.**

The channel coefficient from  $X$  to  $Y$  where  $X, Y \in \{S, D, I\}$  is denoted by  $h_{XY}$ . The channel power gain from  $X$  to  $Y$  is as  $|h_{XY}|^2$ , where  $|\cdot|$  denotes the absolute operation. The channel gain is considered constant during each block; however, it changes independently from one block to another. Here, the environment is assumed to be highly scattered, and the Rician distribution is used to model the  $I \rightarrow D$  channel. The three remaining channels are modeled by the Rayleigh distribution.

In the next section, the system outage probability regarding the energy and data channels outage is computed.

### 3. Outage probability analysis

This section analyzes the outage probability of the proposed model in figure 1. Thus the outage of the data transfer channel is first examined, and then the outage probability of the energy channels of the model is investigated. In addition, the system outage probability is computed based on the obtained energy and data outage relations.

#### 3.1. Outage probability of data channel

Consider  $P_D$  and  $P_I$  as the transmission power of the destination terminal and interference signal, respectively. In the first phase of the transmission block, the source terminal scavenges the broadcasted energy by the destination and also from the ambient interference signals. The aggregate energy at the source can be formulated as:

$$E_S = \alpha T \eta_D P_D |h_{DS}|^2 + \alpha T \eta_I P_I |h_{IS}|^2, \quad (1)$$

where  $\eta_D$  and  $\eta_I$  are the energy harvesting efficiency from the  $DS$  and  $IS$  links, respectively. Thus the source transmit power can be obtained as:

$$P_S = \frac{E_S}{(1-\alpha)T} = \frac{\alpha T \eta_D P_D |h_{DS}|^2 + \alpha T \eta_I P_I |h_{IS}|^2}{(1-\alpha)T} \quad (2)$$

By considering  $\eta_D = \eta_I = \eta$  and  $\rho = \eta \frac{\alpha}{(1-\alpha)}$  can be re-written as:

$$P_S = \rho (P_D |h_{DS}|^2 + P_I |h_{IS}|^2) \quad (3)$$

In the second phase, the powered source transmits data to the destination. Regarding the simultaneous receiving of the interference signal and data, the received signal at the destination can be expressed as:

$$y_D = h_{SD} x_S + h_{ID} x_I + n_d \quad (4)$$

where  $n_d$  is the additive white Gaussian noise (AWGN) with  $n_d \sim \mathcal{N}(0, N_0)$ , where  $N_0$  is the

power spectrum of the white noise. Moreover,  $x_S$  and  $x_I$  are, respectively, the source and the interference signal with  $E\{|x_S|^2\} = P_S$  and  $E\{|x_I|^2\} = P_I$ . By taking the first term in the right-hand side of (4) as a signal and the second and third terms as a noise, the signal to noise ratio at the destination can be formulated as:

$$\gamma_D = \frac{P_S |h_{SD}|^2}{P_I |h_{ID}|^2 + N_0} \quad (5)$$

where regarding (3),  $\gamma_D$  can be re-written as:

$$\gamma_D = \rho \frac{|h_{SD}|^2 (P_D |h_{DS}|^2 + P_I |h_{IS}|^2)}{P_I |h_{ID}|^2 + N_0} \quad (6)$$

In this investigation, the Rician distribution is used to model the  $I \rightarrow D$  channel, while  $I \rightarrow S$ ,  $S \rightarrow D$ , and  $D \rightarrow S$  are modeled by the Rayleigh distribution. For simplicity, it is assumed that  $V = \frac{P_D}{P_I} |h_{DS}|^2 + |h_{IS}|^2$  and  $W = \frac{\rho P_I |h_{SD}|^2}{P_I |h_{ID}|^2 + N_0}$ . For simplicity, we take  $P_D = P_I$ . Thus (6) can be re-written as:

$$\gamma_D = \mathbf{WV} \quad (7)$$

The outage on a data channel happens when the channel's SNR becomes less than a desired threshold. Thus the outage probability of the  $S \rightarrow D$  channel from the system capacity is expressed as:

$$\begin{aligned} \text{OP}_{DT} &= \mathbf{P}((1 - \alpha) \log_2(1 + \gamma_D) \leq R) \\ &= \mathbf{P}(\mathbf{WV} \leq \gamma_{th}) = \int_0^\infty \mathbf{F}_W\left(\frac{\gamma_{th}}{v}\right) f_v(v) dv \end{aligned} \quad (8)$$

where  $\gamma_{th} = 2^{\frac{R}{1-\alpha}} - 1$  denotes the desired threshold SNR value, and  $R$  is the target rate. For solving (8), the CDF of  $W$  and the PDF of  $V$  should be first computed. These functions are calculated in the Appendix section.

Based on the relations obtained in the Appendix section, we have:

$$\begin{aligned} \mathbf{F}_W\left(\frac{\gamma_{th}}{v}\right) &= e^{-K_{ID}} \sum_{n=0}^\infty \frac{(K_{ID})^n}{(n+1)!} (\mathbf{a}_{ID})^{n+1} \times \\ &\left[ \frac{1}{\mathbf{a}_{ID}} - \frac{e^{-\frac{\gamma_{th} N_0}{v \rho K_{SD} P_I}}}{\left(\frac{\gamma_{th}}{v \rho K_{SD}} + \mathbf{a}_{ID}\right)} \right] \end{aligned} \quad (9)$$

where  $\lambda_{ID}$  is the mean received power from all paths,  $K_{ID} = \frac{\vartheta^2}{2\sigma^2}$  denotes the ratio of the power of the line-of-sight path to the power of non-line-of-sight paths, and  $\mathbf{a}_{ID} = \frac{1+K_{ID}}{\lambda_{ID}}$ . Moreover, the function  $f_v(v)$  is obtained in the Appendix section. Thus (8) can be re-written as:

$$\begin{aligned} \text{OP}_{DT} &= e^{-K_{ID}} \sum_{n=0}^\infty \frac{(K_{ID})^n}{(n+1)!} (\mathbf{a}_{ID})^n \left[ \frac{1}{2K_{DS}} - \right. \\ &\left. \frac{1}{K_{DS}^2} \int_0^\infty \left( \frac{v^2}{v + \frac{\gamma_{th}}{\rho K_{SD} \mathbf{a}_{ID}}} \right) e^{-\frac{v}{K_{DS}} - \left( \frac{\gamma_{th} N_0}{v \rho K_{SD} P_I} \right)} dv \right] \end{aligned} \quad (10)$$

It should be noted that  $K_{IS}$  and  $K_{DS}$  are the mean of signal over  $I \rightarrow S$  and  $D \rightarrow S$  links, respectively, and are assumed equal in deriving the outage of the data channel  $S \rightarrow D$ . Solving the integral in (10) to reach a closed-form solution is complex. For that,  $OP_{DT}$  is computed numerically.

**3.2. Outage probability of energy channels**

The source terminal harvests energy from both the destination and interference signals, as demonstrated in figure 1. Similar to the data channels, the energy channels may experience an outage. Whenever the energy of a transmitter is less than the required amount for transmission, the data is received with error at the receiver with a high probability. In other words, an energy outage occurs at the transmitter. As an outage in the energy harvesting channels affects the data transfer, it is essential to be considered in the system outage analysis. The energy outage probability of a terminal whose harvest energy is  $E$  is defined as [15]:

$$OP_{EH} = P(E \leq \theta_{th}) \tag{11}$$

where  $\theta_{th}$  is the minimum required energy for data transmission. In our model depicted in figure 1 (a), the aggregate energy at the source via harvesting is shown in (1). Thus the energy outage probability at the source is formulated as:

$$OP_{EH} = P(E_S \leq \theta_{th}) = P\left(V \leq \frac{\theta_{th}}{\alpha T \eta P_I}\right) = F_V\left(\frac{\theta_{th}}{\alpha T \eta P_I}\right) \tag{12}$$

where according to the  $F_V(b)$  obtained in the Appendix section, we have:

$$OP_{EH} = 1 - \left(1 + \frac{\theta_{th}}{\alpha T \eta P_I K_{SD}}\right) e^{-\frac{\theta_{th}}{\alpha T \eta P_I K_{SD}}} \tag{13}$$

**3.3. System outage probability**

The total system consists of both energy and data channels working independently. The outage at the energy harvesting and the data transfer channels leads to a system outage. If the harvested energy from the destination and interference signals is very high and intermittent, the energy outage probability approaches zero. Thus the outage in the system occurs when there is an outage in data transfer channels; in other words:

$$OP_{sys} = OP_{DT} \tag{14}$$

However, the more realistic case is when the fluctuation in the harvested energy is considered. Thus to have a more reliable amount of harvested energy in the proposed model, it is considered the

energy provided via two separate channels. In this way, the sum of harvested energies is more probable to meet the required energy of the source compared to the case that energy is provided via only one link. In this case, the system outage probability is given by:

$$OP_{sys} = OP_{EH} + (1 - OP_{EH})OP_{DT} \tag{15}$$

**4. A Special case: One energy harvesting channel**

This section examines a special case of the proposed model in figure 1 (a). In this case, it is assumed that the source energy is harvested only via the  $D \rightarrow S$  link, and the aim is to investigate how much the system performance degrades. With regard to the Rayleigh distribution model of the energy channel, we have  $f_V(b) = \frac{1}{K_{DS}} e^{-\frac{b}{K_{DS}}}$ . Thus the outage probability of the data transfer channel is given by:

$$OP_{DT} = e^{-K_{ID}} \sum_{n=0}^{\infty} \frac{(K_{ID})^n}{(n+1)n!} (a_{ID})^n \left[ \frac{1}{K_{DS}^2} - \frac{1}{K_{DS}} \int_0^{\infty} \left( \frac{v}{v + \frac{\gamma_{th}}{\rho K_{SD} a_{ID}}} \right) e^{-\frac{v}{K_{DS}} - \left( \frac{\gamma_{th} N_0}{v \rho K_{SD} P_I} \right)} dv \right] \tag{16}$$

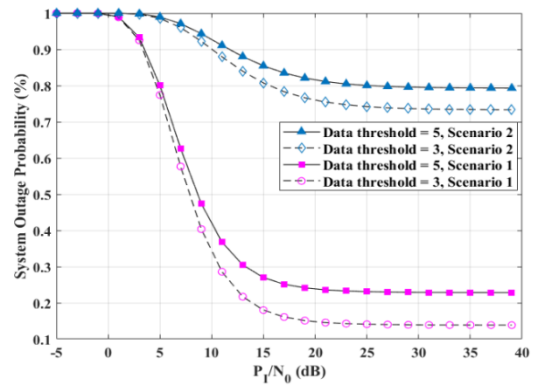


Figure 2. System outage performance versus radiated energy power for  $\alpha = 0.5$  and  $K = 1$ .

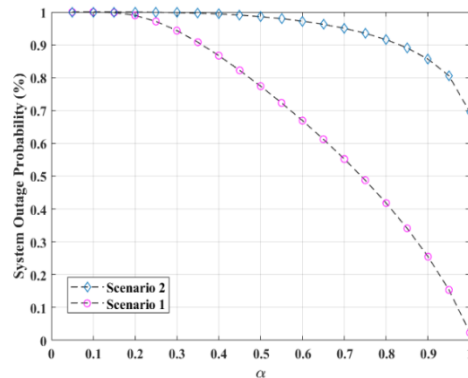


Figure 3. System outage performance versus  $\alpha$  for  $\gamma_{th} = 3$  and  $K = 1$ .

and the energy outage is obtained as:

$$OP_{EH} = F_V\left(\frac{\theta_{th}}{\alpha T \eta P_1}\right) = 1 - e^{-\frac{\theta_{th}}{\alpha T \eta P_1 K_{SD}}} \quad (17)$$

The system outage is also computed based on (15)

### 5. Computer simulations

Computer simulations using Matlab are conducted in order to evaluate the performance of the proposed model. Two cases are considered, the case in which two energy harvesters for the source are applied, namely scenario 1, and the case with one energy harvesting link, namely scenario 2. Unless otherwise specified, the system parameters are chosen as  $\eta = 0.8$  and transmission block time  $T = 1$ . The parameters of Rician distribution are  $K_{ID} = 0.2$  and  $a_{ID} = 1.2$ . On the other hand, the values of different parameters including  $\alpha$ ,  $\gamma_{th}$ , and  $K$  are varied during various simulations. It should be noted that for the Rayleigh channels, we assume  $K_{DS} = K_{SD} = K_{IS} = K$ .

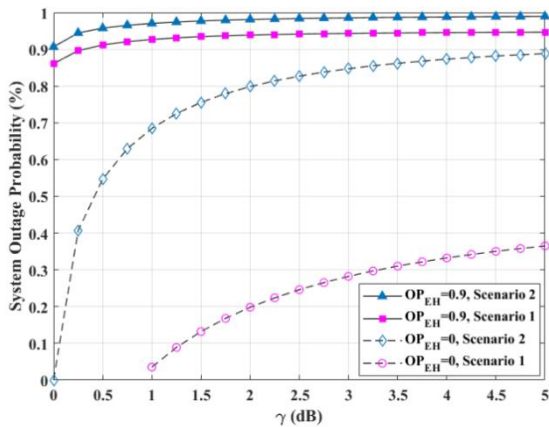


Figure 4. System outage performance versus data threshold for  $K = 1$  and  $\frac{P_I}{N_0} = 5$  dB.

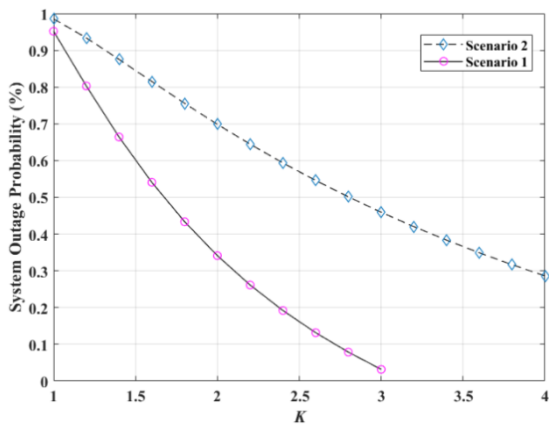


Figure 5. System outage performance versus  $K$  for  $\alpha = 0.5$ ,  $\gamma_{th} = 3$  and  $\frac{P_I}{N_0} = 5$  dB.

Figure 2 plots the system outage probability of scenarios 1 and 2 with respect to  $\frac{P_I}{N_0}$  for different values of data threshold and  $\alpha = 1$ . It can be observed that the outage in the system with one energy harvester (scenario 2) is higher than in the system with two energy harvesting channels. In addition, it is demonstrated that the increase in the radiated power of energy sources results in a significant reduction in the system outage in the low SNR (up to 15 dB) regime. After approximately 15 dB, the system outage converges to a constant value, where for scenario 1 it is about 0.15, while it is 0.75 in scenario 2. Moreover, the system outage probability in the low data threshold is observed to be less than the case with a high data threshold.

The system outage probability of scenarios 1 and 2 under different values of  $\alpha$  is compared in figure 3, and the parameters are set to  $\gamma_{th} = 3$  and  $K = 1$ . With the increase of  $\alpha$  from zero to one, the outage in both scenarios decreases; however, the model in scenario 1 outperforms the one in scenario 2, especially in high values of  $\alpha$ .

Figure 4 represents the system outage of both scenarios with respect to the data threshold, while the energy outage probability is fixed at 0 and 0.9. Other parameters are chosen as  $K = 1$  and  $\frac{P_I}{N_0} = 5$  dB. When there is no outage in energy channels, the system outage occurs due to the outage in the data channel. Moreover, figure 4 demonstrates that the least system outage in each scenario is when the outage probability of energy channels is zero. For example, when the probability of energy outage channels increases, the system outage increases from 0.2 to 0.93 in scenario 1 for data threshold 2. However, it changes from 0.8 to 0.98 in scenario 2. In addition, an increasing trend in the system outage is observed in all curves by the increase of the data threshold.

In figure 5, the values for  $\alpha = 0.5$ ,  $\gamma_{th} = 3$  and  $\frac{P_I}{N_0} = 5$  dB are fixed, and the effect of  $K$  on the system outage performance in both scenarios is investigated. The rise of  $K$  from 1 to 4 leads to a gradual decrease in the outage of scenario 2, while the outage improvement in scenario 1 is faster.

### 6. Conclusion

This paper addresses the outage probability analysis for the energy harvesting assisted WPCN in the presence of interference signals. It was assumed that the source did not have any internal energy supply. In scenario 1, the source required transmission energy was harvested via both the

$D \rightarrow S$  and  $I \rightarrow S$  channels. In addition to the data channel outage analysis, the outage of energy channels was analysed; then, based on them, the outage probability of the system was obtained. Several simulations were conducted in order to evaluate the outage performance of the proposed model. The results obtained were compared with the case where the source harvested energy via only the  $DS$  channel (scenario 2). Comparing the two scenarios' results demonstrated that the system outage highly degraded when the required energy of the source was provided via two channels. Moreover, the system outage is highly affected by the energy outage. The lower energy outage leads to a decrease in the system outage.

### 7. Appendix

Let consider  $z_1 = |h_{DS}|^2$ ,  $z_2 = |h_{IS}|^2$ ,  $z_3 = |h_{SD}|^2$ , and  $z_4 = |h_{ID}|^2$ . Based on these definitions, the functions  $F_W(b)$ ,  $F_V(b)$ , and  $f_V(b)$  are calculated in this section.

- First, we compute  $F_W(b)$  as

$$F_W(\mathbf{b}) = P(\mathbf{W} \leq \mathbf{b}) = P\left(\frac{\rho z_3}{z_4 + \frac{N_0}{P_1}} \leq \mathbf{b}\right) = P\left(z_3 \leq \frac{b N_0}{\rho P_1} \left(\frac{P_1}{N_0} z_4 + 1\right)\right) = \int_0^\infty F_{z_3}\left(\frac{b N_0}{\rho P_1} \left(\frac{P_1}{N_0} z_4 + 1\right)\right) f_{z_4}(z_4) dz_4 \quad (18)$$

The CDF of Rayleigh distribution and the PDF of Rician distribution are, respectively, as:

$$F_{z_3}(z_3) = 1 - e^{-\frac{z_3}{K_{SD}}} \quad (19)$$

$$f_{z_4}(z_4) = e^{-K_{ID}} \sum_{n=0}^{\infty} \frac{(K_{ID})^n}{(n!)^2} (a_{ID})^{n+1} z_4^n e^{-(a_{ID} z_4)} \quad (20)$$

Thus based on (19) and (20), (18) can be re-written as:

$$F_W(\mathbf{b}) = e^{-K_{ID}} \sum_{n=0}^{\infty} \frac{(K_{ID})^n}{(n!)^2} (a_{ID})^{n+1} \int_0^\infty \left(1 - e^{-\frac{1}{K_{SD}} \left(\frac{b z_4}{\rho} + \frac{b N_0}{\rho P_1}\right)}\right) z_4^n e^{-(a_{ID} z_4)} dz_4 \quad (21)$$

By applying [16, p. 3.326.2], (21) can be formulated as:

$$F_W(\mathbf{b}) = e^{-K_{ID}} \sum_{n=0}^{\infty} \frac{(K_{ID})^n}{(n!)^2} (a_{ID})^{n+1} \left[ \frac{1}{a_{ID}} - \frac{e^{-\frac{b N_0}{\rho K_{SD} P_1}}}{\left(\frac{b}{\rho K_{SD}} + a_{ID}\right)} \right] \quad (22)$$

- Next, to derive  $F_V(b)$  and  $f_V(b)$ , we have:

$$F_V(\mathbf{b}) = P(\mathbf{V} \leq \mathbf{b}) = P(\mathbf{z}_1 + \mathbf{z}_2 \leq \mathbf{b}) = P(\mathbf{z}_1 \leq \mathbf{b} - \mathbf{z}_2) = \int_0^b f_{z_2}(z_2) \int_0^{b-z_2} f_{z_1}(z_1) dz_1 dz_2 \quad (23)$$

With regard to the PDF of Rayleigh distribution as  $f_z(z) = 1 - e^{-\frac{z}{K}}$ , (23) can be re-written as:

$$F_V(\mathbf{b}) = 1 - e^{-\frac{b}{K_{DS}}} - b \frac{e^{-\frac{b}{K_{DS}}}}{K_{DS}} \quad (24)$$

Regarding that,  $K_{IS} = K_{DS}$ . In this case, the PDF of  $V$  can be simply obtained from (24) as:

$$f_V(\mathbf{b}) = \frac{b}{K_{DS}^2} e^{-\frac{b}{K_{DS}}} \quad (25)$$

### 8. References

- [1] Bi S., Ho, C. K., and Zhang, R. (2015). Wireless powered communication: opportunities and challenges, IEEE Communications Magazine, Vol. 53, No. 4, pp. 117–125.
- [2] Niyato, D., Kim, D. I. Maso, M., and Han, Z. (2017). Wireless Powered Communication Networks: Research Directions and Technological Approaches. IEEE Wireless Communications, Vol. 24, No. 6, pp. 88-97.
- [3] Bi, S., Zeng, Y., and Zhang, R. (2016). Wireless powered communication networks: An overview. IEEE Wireless Communications, Vol. 23, no. 2, pp. 10–18.
- [4] Ju, H. and Zhang, R. (2013). Throughput Maximization in Wireless Powered Communication Networks. In IEEE Transactions on Wireless Communications, Vol. 13, No. 1, pp. 418-428.
- [5] Deepan N. and Rebekka, B. (2019). On the performance of wireless powered communication networks over generalized  $\kappa$ - $\mu$  fading channels. Physical Communication, Vol. 36, p. 100759.
- [6] Ju, H. and Zhang, R. (2014). User cooperation in wireless powered communication networks. 2014 IEEE Global Communications Conference, Austin, TX, pp. 1430-1435.
- [7] Zhong, C., Chen, X., Zhang, Z., and Karagiannidis, G. K. (2015). Wireless-Powered Communications: Performance Analysis and Optimization. In IEEE Transactions on Communications, Vol. 63, No. 12, pp. 5178-5190.
- [8] Masood, Z., Jung, S. P., and Choi, Y. (2018). Energy-Efficiency Performance Analysis and Maximization Using Wireless Energy Harvesting in Wireless Sensor Networks. Energies, Vol. 11, No. 11, p. 2917.
- [9] Tan, N. Nguyen, T. H. Q. Minh, P. Tran, T., and Miroslav Voznak. (2018). Energy Harvesting over Rician Fading Channel: A Performance Analysis for Half-Duplex Bidirectional Sensor Networks under Hardware Impairments. Sensors, Vol. 18, No. 6, p. 1781.
- [10] Van-Duc, P., Nguyen, T. N., Tran, M., Trang, T. T., Voznak, M., Ha, D. H., and Nguyen, T. L. (2019). Power Beacon-Assisted Energy Harvesting in a Half-Duplex Communication Network under Co-Channel Interference over a Rayleigh Fading Environment:

Energy Efficiency and Outage Probability Analysis. *Energies*, Vol. 12, No. 13, p. 2579.

[11] Huang, C., Zhou, S., Xu, J., Niu Z., Zhang, R., and Cui, S. *Energy harvesting wireless communications*. John Wiley and Sons, 2018.

[12] Chen, Z., Cai, L. X., Cheng, Y., and Shan, H. (2017). Sustainable cooperative communication in wireless powered networks with energy harvesting relay, *IEEE Transactions on Wireless Communications*, Vol. 16, No. 12, pp. 8175–8189.

[13] Zhou, X., Ho, C. K., and Zhang, R. (2016). Wireless power meets energy harvesting: a joint energy allocation approach in OFDM-based system. *IEEE Transactions on Wireless Communications*, Vol. 15, No. 5, pp. 3481–3491.

[14] Veilleux, S., Bundy, K., Almaghasilah, A., and Abedi, A. (2018). Transmission scheduling for wireless energy transfer with dual data-energy channel models. In 2018 6th IEEE International Conference on Wireless for Space and Extreme Environments (WiSEE), Huntsville, AL, USA, pp. 30–35.

[15] Naderi, S., Khosroazad, S., and Abedi, A. (2022). Relay-Assisted Wireless Energy Transfer for Efficient Spectrum Sharing in Harsh Environments. *International Journal of Wireless Information Networks*, pp. 1-10.

[16] Gradshteyn, I. S. and Ryzhik, I. M., *Table of integrals, series, and products*, 8th ed. Academic Press, Elsevier Inc., 2014.